

CrystEngComm

Accepted Manuscript



This is an *Accepted Manuscript*, which has been through the Royal Society of Chemistry peer review process and has been accepted for publication.

Accepted Manuscripts are published online shortly after acceptance, before technical editing, formatting and proof reading. Using this free service, authors can make their results available to the community, in citable form, before we publish the edited article. We will replace this *Accepted Manuscript* with the edited and formatted *Advance Article* as soon as it is available.

You can find more information about *Accepted Manuscripts* in the [Information for Authors](#).

Please note that technical editing may introduce minor changes to the text and/or graphics, which may alter content. The journal's standard [Terms & Conditions](#) and the [Ethical guidelines](#) still apply. In no event shall the Royal Society of Chemistry be held responsible for any errors or omissions in this *Accepted Manuscript* or any consequences arising from the use of any information it contains.

Encapsulated Cd₃P₂ Quantum Dots Emitting from the Visible to the Near Infrared for Bio-labelling Applications

Liping Ding,[†] Shulian He,[†] Dechao Chen,[†] Mei Huang,[†] Jinzhang Xu,[†] Stephen G. Hickey,[‡] Alexander Eychmüller,[‡] Shu-Hong Yu,[§] and Shiding Miao^{†}*

[†] Anhui Key Lab of Controllable Chemical Reaction & Material Chemical Engineering, School of Chemical Engineering, Hefei University of Technology, Tunxi Road. 193, Hefei, Anhui Prov., 230009 China

[‡] Physical Chemistry, TU Dresden, Berg Str. 66b, Dresden, D-01062, Germany

[§] Division of Nanomaterials and Chemistry, Hefei National Laboratory for Physical Sciences at Microscale, Department of Chemistry, University of Science and Technology of China, Hefei 230026, China

The Cd₃P₂ quantum dots (QDs) have been synthesized in both aqueous and high boiling point surfactant solutions via a gas-bubbling method. The synthesized QDs exhibit photoluminescent wavelengths spanning across the visible red to the near-infrared (NIR) spectral region. Two types of shell materials, SiO₂ nano-beads and PS micro-spheres, have been employed to encapsulate the Cd₃P₂ QDs which provide protecting layers from the physiological solutions. The coating layers are proven to enhance the optical and chemical stability of Cd₃P₂ QDs, and make the fluorescent particles capable of sustaining long-term photo-oxidation. To demonstrate the applicability of the bio-labelling, the fluorescent composite particles (PS@QDs, SiO₂@QDs)

were injected into a culture medium of colorectal carcinoma (LoVo) cells. The result demonstrates that the PS@QDs exhibits a brighter fluorescence, but SiO₂@QDs provides a better photo-stability which consequently led to long-term cancer cell detection as well as a much lower release of toxic Cd²⁺ into the PBS solutions.

1. Introduction

The goal of attaining fluorescent probes whose emission wavelengths span from the visible red to the near-infrared (NIR) i.e. across the so-called tissue optical window (from 700 to 1400 nm) has been stimulated in great part by the specific interest of employing them for in-vivo biological imaging.¹ A most promising fluorescent probe category is that of semiconductor nanocrystals (NCs) whose average size is below the Bohr radius of the excitons in their bulk materials, as in such NCs the emission wavelength can often be significantly varied as a function of the average size to form quantum dots (QDs). Cadmium phosphide (Cd₃P₂) is a prominent II-V semiconductor which features a narrow direct optical band-gap of ~0.65 eV,² relatively high dielectric constant (5.8),³ large exciton Bohr radius (~36 nm),^{4,5,6} large effective Stokes shift, and a small effective mass of the electron (0.05m_e).^{7,8,9} This combination of properties has been substantiated to provide Cd₃P₂ with wide spectral tunability (~460-1600 nm), to convey a narrow emission spectral window in the case where a uniform size distribution is obtained, and due to the large Stokes shift a means by which the re-adsorption of light can be avoided. These properties afford Cd₃P₂ an exceptional position as a candidate in such applications as photovoltaics,¹⁰ LEDs,² and bio-labelling.^{11,12,13} However, the toxicity and instability of Cd₃P₂ QDs have not been well documented if they are to be used in biological applications. Therefore,

it is of immense significance to develop a method or coating materials that make Cd_3P_2 applicable in biological environments.¹⁰

Innovations in colloidal chemistry over the last decades have enabled the embedding QDs in a shell material and their subsequent use for the imaging of bio-tissues.^{14,15} Dispersion polymerization is an attractive technique for producing uniform micro-spheres with diameters of between 0.5-10 μm due to its single-step process.¹⁶ Synthesis of monodisperse polymer spheres of micrometer-size has drawn great interest, and the incorporation of externally situated nanoparticles into these micro-spheres is particularly attractive and challenging.^{17,18} For example, polystyrene (PS) micro-spheres have been investigated due to their potential application within the biomedical field.¹⁹ Up to now, PS micro-spheres have been used to encapsulate CdSe ,²⁰ CdSe/ZnS ,²¹ Au nanoparticles,²² amongst others.²³ The preparative procedures include microemulsion polymerization,²⁴ emulsifier-free polymerization,²⁵ seed emulsion polymerization²⁶ and dispersion polymerization.^{27,28} Silica (SiO_2), which has proven itself to be another bio-friendly material, can be also used to encapsulate QDs providing a number of advantages amongst which can be found: the surface chemistry of the QDs can be altered, the solubilization of the materials in bio-solutions can be facilitated, and the toxicity can be avoided, etc.^{29,30} The fabrication of QDs containing SiO_2 beads has been previously reported. For example, II-VI QDs possessing functional alkoxides have been employed as an efficient means by which the QDs may be encapsulated by SiO_2 shells.^{31,32} These type of composite QDs have also been demonstrated to work as a means of monitoring organs in-vivo, e.g., CdHgTe/SiO_2 NCs in the mouse model.³³ However, difficulties are encountered when the different types of QDs are to be encapsulated. For example, oil dispersible QDs which have been synthesized using the hot-injection methodology require further surface treatments before their coating procedures

can be successfully applied.³⁴ In some cases, the core/shell structure or transition metal doped QDs were designed so as to be buried inside silica to protect the photoluminescence.^{35,36} These unknown obstructions to the coating of QDs possessing a variety of surface chemistries that originate from different experimental procedures provided the motivation for us to undertake the further studies outlined below.

In this work, Cd₃P₂ QDs of different average sizes were synthesized both in aqueous solutions and high-temperature surfactant solutions via a gas-bubbling method. The Cd₃P₂ QDs so synthesized exhibit emission wavelengths that span across the visible red to the near-infrared (NIR) spectral region. The primary purpose of this study is to improve the biocompatibility and stability of Cd₃P₂ QDs as well as weaken the impact of the potential toxicity of Cd₃P₂ QDs when used for bio-labelling. Two types of shell materials, SiO₂ nano-beads and PS micro-spheres, are employed to encapsulate the Cd₃P₂ QDs which provide protecting layers from the physiological solutions. The coating layers are proven to enhance the stability of Cd₃P₂ QDs, and make the fluorescent particles capable of sustaining long-term photo-oxidation. To demonstrate the applicability of the bio-labelling, the prepared fluorescent particles were injected into a culture medium of colorectal carcinoma (LoVo) cells. The result demonstrates that the fluorescent composite of PS@QDs exhibits a brighter fluorescence, but SiO₂@QDs provides a better photo-stability which consequently led to long-term cancer cell detection as well as a much less release of toxic Cd²⁺ into the PBS solutions.

2. Experiment section

2.1 Chemicals

Styrene monomer and divinylbenzene (DVB) were purchased from Aldrich Chemical Co. and washed with 10% aqueous sodium hydroxide solution and DI water to remove the inhibitor. Azodiisobutyronitril (AIBN), polyvinylpyrrolidone (PVP), tetraethylorthosilicate (TEOS), $\text{Cd}(\text{ClO}_4)_2$, mercaptopropionic acid (MPA), Ca_3P_2 , $\text{NH}_3 \cdot \text{H}_2\text{O}$ solution and ethanol were purchased from Sinopharm Chemical Regent Co. China and used without further purification. Cadmium oleate ($\text{Cd}(\text{OA})_2$) was synthesized from cadmium oxide and oleic acid in 1-octadecene (ODE) solution according to the reported literature.¹

2.2 Preparation of Cd_3P_2 QDs

Cd_3P_2 QDs are synthesized according to our reported methods and that of Weller.^{1, 2} For the aqueous synthesis, Cd_3P_2 QDs were prepared using an ex-situ produced PH_3 gas which was bubbled through $\text{Cd}(\text{ClO}_4)_2/\text{MPA}/\text{H}_2\text{O}$ solution. The synthesis was carried out in a four-necked flask connected with a column containing Ca_3P_2 which is used to produce the PH_3 gas ($\text{Ca}_3\text{P}_2 + \text{H}_2\text{SO}_4$). The precursor solution in the four-necked flask includes $\text{Cd}(\text{ClO}_4)_2$ (0.1008g), MPA (0.063g) and water (10 mL). The pH value is maintained at between 10 and 12 by the addition of NaOH solution (0.1 M). The PH_3 gas was bubbled through the precursors using a flow of N_2 as the carrier. The colorless mixture changes to orange red within 10 min of the initialisation of the gas-bubbling which suggests the formation of colloidal Cd_3P_2 QDs. The resulting NCs emitting in the visible region (yellow to dark red) were collected and purified by first precipitating employing ethanol as non-solvent, and then re-dispersion in water to remove any unreacted ions. For the preparation of Cd_3P_2 QDs emitting in the NIR region, the procedures were conducted similarly except that the aqueous solution was replaced by hot-surfactant solution (ODE, TOPO and $\text{Cd}(\text{OA})_2$) where higher temperatures can be applied ($T > 100^\circ\text{C}$,

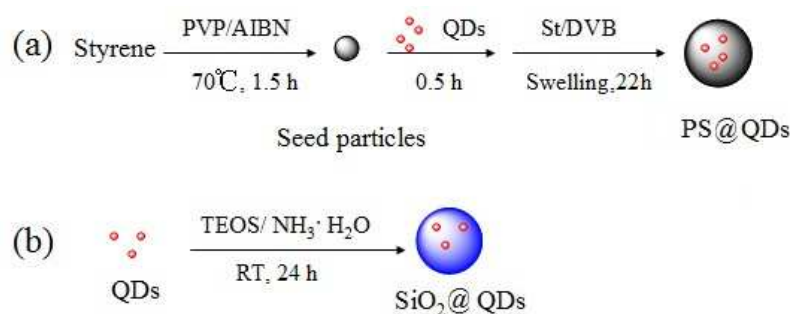
reaction time >30 min).¹ To convert the TOPO capped QDs to water-soluble QDs ligand-exchange experiments were conducted in which the TOPO-coated QDs were added to a solution of methanol and MPA. The amount of MPA used is ~200% the amount of TOPO used in the initial synthesis. The pH value of the mixture was adjusted to ~11 using a KOH/methanol solution (0.1 M). After 2 hrs of stirring, these particles were separated by centrifugation. Subsequent re-dispersion of the particles into water then yielded a clear and non-scattering solution.

2.3 Synthesis of Cd₃P₂ QDs@ PS Micro-spheres

The standard protocol for the two-stage copolymerization of QDs and styrene is listed in Table S1 in the supporting information.²⁸ Briefly, the desired amount of the stabilizer divinylbenzene (PVP), initiator azodiisobutyronitril (AIBN) and the monomer styrene were loaded into a 25 mL three-neck reaction flask equipped with a condenser and a gas inlet. After homogenization the solution was deoxygenated by bubbling it with nitrogen gas for at least 30 min. The dispersion was then heated to 70°C and DVB was added while the dispersion was kept stirring. After a polymerization period of 1.5 hrs, 300 µL Cd₃P₂ QDs in aqueous solution whose absorbance is ~0.4 units at the first excitonic peak was added. The QDs were then adsorbed onto the surface of the particles. After about 0.5 hrs, another portion of styrene and DVB solution was added into the mixture. The QDs were subsequently coated by the further growth of PS. After stirring for 24 hrs, the product was collected and washed twice with deionized water and ethanol. The final product PS@QDs micro-spheres were vacuum-dried at 50°C. The synthetic scheme is shown in Scheme 1.

2.4 Synthesis of SiO₂@QDs

The SiO₂@QDs nanoparticles were prepared by adapting a modified Stöber method,³⁷ which involves the hydrolysis and condensation of tetraethyl orthosilicate (TEOS) in the presence of aqueous ammonia. Typically, the TEOS (200 μL) and QDs solution (200 μL, Abs (first peak) = ~0.4 unit) were mixed with 4 mL anhydrous ethanol. After magnetically stirring for 20 min, 300 μL of ammonia (28% in H₂O) and 4 mL ethanol were added. The reaction was maintained for 24 hrs under magnetic stirring. The product (SiO₂@QDs) was obtained by centrifugation, and was washed three times with water and ethanol sequentially followed by vacuum-drying. The schematic of the both procedures is denoted in Scheme 1.



Scheme 1 (a) Schematic presentation for the synthesis of PS@QDs in ethanol/water via a two-stage copolymerization, and (b) SiO₂@QDs via a modified Stöber method

2.5 Cell labelling

LoVo cells (ATCC cell line, Jiniou Bio-Tec Corp., Guangzhou, China) were cultivated according to a reported method.³⁸ The composite QD particles were delivered into the cells via endocytosis.³⁹ Typically, the LoVo cells were cultured at 37°C in 5% CO₂/95% air in GIBCO supplemented with 10% fetal bovine serum (FBS, Jiniou Bio-Tec Corp.) and 1% penicillin/streptomycin. Afterwards the cells were incubated for a period of time, fixed at room temperature for 15 min (4% paraformaldehyde, 0.1% glutaraldehyde in PBS), and incubated with

0.15% diaminobenzidine in PBS (pH=7.4) for 15 min. Fluorescence particles (Cd_3P_2 QDs, $\text{SiO}_2@\text{QDs}$ and $\text{PS}@\text{QDs}$) were added to cells at 80-90% confluency and incubated for a period of time at 37°C . The labelled cells were then washed by removing the PBS and replacing it with fresh PBS three times, along with a slight agitation in each wash step to remove any QDs that were not taken up by cells.

2.6 Characterizations

The morphology and micro-structure were examined by scanning electron microscopy (SEM, SV8020, Hitachi) and transmission electron microscopy (TEM, JEM-2100F). The SEM samples were prepared with a small amount of powder on a copper plate. To observe the QDs encapsulated in the micrometer-sized PS or SiO_2 spheres, the composite was embedded in epoxy resin to form a solid specimen, and the specimen then cut with an ultramicrotome to obtain an ultrathin section of the micro-spheres, which was examined by TEM observation. The X-ray diffraction profiles were collected on an X-ray diffractometer (D/MAX2500V) operated at 40 kV. Absorbance spectra were recorded by using a Cary D5000 UV-Vis-NIR spectrophotometer (Varian) equipped with a quantum yield integrating sphere. Photoluminescence (PL) measurements were performed on a Horiba Jobin Yvon FluoroLog-3 spectrofluorometer at a spectral resolution of 1.0 nm. Fluorescence microscopy was carried out using an inverted fluorescence microscope (IX-70, OLYMPUS) equipped with an Hg excitation lamp and a true-colour digital camera. To probe the concentration of Cd^{2+} that is released into the PBS solution during incubation, the solution was analyzed by atomic absorption spectroscopy (AAS, Optical 7300DV, PerkinElmer), and a standard curve with known concentrations (0.1, 0.5, 1, 2, 5 $\mu\text{g}/\text{mL}$) is applied.

3. Results and discussion

3.1 Optical Properties Study

Fig. 1a displays the absorbance (Abs), photoluminescence (PL) and photoluminescence excitation (PLE) spectrum of the uncoated Cd_3P_2 QDs, the $\text{PS}@ \text{Cd}_3\text{P}_2$ and $\text{SiO}_2@ \text{Cd}_3\text{P}_2$ composites. Due to the ease of dispersing the MPA coated QDs in water, we measured aqueous solutions of the QDs in quartz cells in transmission mode. Because the $\text{PS}@ \text{Cd}_3\text{P}_2$ and $\text{SiO}_2@ \text{Cd}_3\text{P}_2$ composites cannot be dispersed in any solvent without giving strongly scattering, the spectra of $\text{PS}@ \text{Cd}_3\text{P}_2$ and $\text{SiO}_2@ \text{Cd}_3\text{P}_2$ composites were measured in reflection mode by using an integrating sphere. It is found that the Abs profile of Cd_3P_2 QDs exhibit more than one peaks in the region between 420 and 500 nm (Fig. 1a, black curve), which suggests that the prepared Cd_3P_2 sample is composed of multiple types of clusters or NCs of different sizes. However, due to the inherent limit of the reaction temperature ($<100^\circ\text{C}$), the clusters which are synthesized using the water-bubbling method always possess an average size of less than 4.0 nm.² This is why the Cd_3P_2 QDs prepared by aqueous-bubbling always exhibit a reddish colour under illumination by UV light. The PL spectrum recorded under excitation at 400 nm is displayed as a green profile in Fig. 1a. A main PL peak at about 610 nm and a weak one at ~ 460 nm are found. According to the previous reports, the PL peak at about 610 nm i.e. the red emitting Cd_3P_2 materials are nanosized QDs with an average size of ~ 3.5 nm. However the 460 nm emission derives from the so-called magic-sized clusters (MSCs).^{2, 40} The PLE spectrum recorded at 610 nm is also shown in Fig. 1a as a pink curve where one can find onsets in the regions from 420 to 480 nm. The PLE spectrum resembles Abs profile reasonably well, which further suggests the red emitting Cd_3P_2 sample contains MSCs and nanosized QDs. For the composite solid samples of $\text{PS}@ \text{Cd}_3\text{P}_2$ or $\text{SiO}_2@ \text{Cd}_3\text{P}_2$, a thick background and Abs spectra

profiles with a high intensity of features could be observed, as shown by the red and blue curves in Fig. 1a, which are due to the uncorrected scattering by the micrometer-sized shells. However, the onset at about 440 nm could still be discerned from these solid samples (denoted by an arrow). The peak corresponds well with the Cd_3P_2 QDs measured in aqueous solution and this observation demonstrates that we have been able to successfully encapsulate the Cd_3P_2 QDs into the composite. The PL spectra of $\text{SiO}_2@\text{Cd}_3\text{P}_2$ and $\text{PS}@\text{Cd}_3\text{P}_2$ are shown in Fig. 1b and 1c, respectively. To confirm the presence of Cd_3P_2 QDs in the composite, the samples were excited with different wavelength (350, 400 and 450 nm). The same PL emission was also received from the peak at ~ 610 nm, which suggests that the emission at 610 nm is indeed from QDs buried in the composite. However, there is a broad peak in region of 420-450 nm in sample of $\text{PS}@\text{Cd}_3\text{P}_2$, which can be attributed to the polymer coating layers.^{41,42} Photographs of the $\text{SiO}_2@\text{Cd}_3\text{P}_2$ and $\text{PS}@\text{Cd}_3\text{P}_2$ materials show that the powders exhibit strong red fluorescence under UV light. Photographs of the composite sample under illumination by a UV lamp (~ 365 nm) are given as insets in Fig. 1b and 1c, respectively which, in conjunction with the fluorescence spectra, demonstrate that the optical properties of the QDs are preserved. Fig. 1d displays the Abs and PL spectra for NIR emissive Cd_3P_2 QDs of ~ 6.0 nm in size,² and their corresponding composites. The emission wavelength of the Cd_3P_2 QDs is found to be at around 1070 nm. The PL peak of $\text{PS}@\text{Cd}_3\text{P}_2$ is found to have shifted a little bit to longer wavelengths, and to be broader than Cd_3P_2 QD cores, which suggests the NIR emission mainly comes from the Cd_3P_2 and the observed broadening phenomenon can be explained by the conjugative effect between the QDs and PS polymer.²¹ Although the sample of $\text{SiO}_2@\text{Cd}_3\text{P}_2$ exhibits a weaker PL peak, the PL peak at the NIR region is still observable, which demonstrates the successful encapsulation of the QDs in SiO_2 .

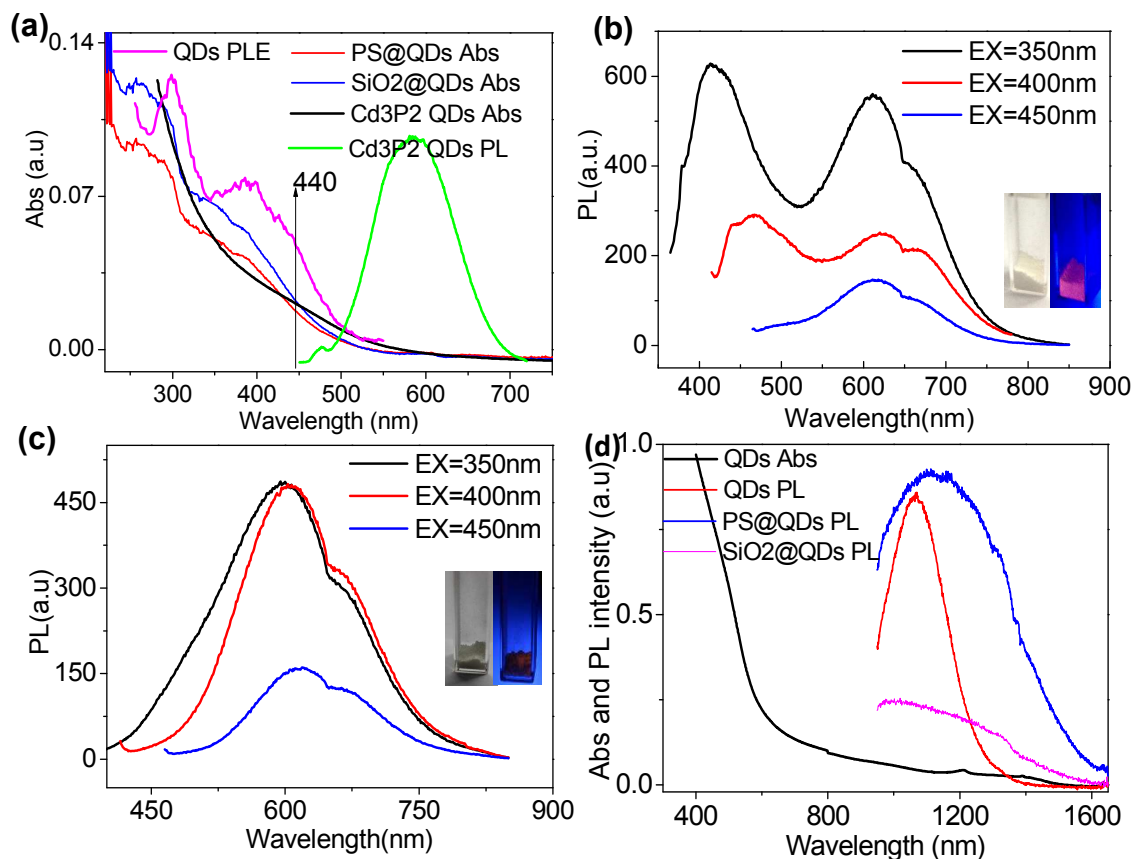


Fig. 1 (a) Abs, PL and PLE spectra of Cd₃P₂ QDs, PS@QDs and SiO₂@QDs; (b) PL spectra of PS@QDs excited with different wavelengths; Insets are photographs of powders under illumination by daylight (left tubes) and UV light of ~365 nm (right). (c) PL spectra of SiO₂@QDs excited with different wavelengths and the corresponding photographs under illumination by daylight and UV light and (d) Abs and PL spectra of Cd₃P₂ QDs, SiO₂@QDs and PS@QDs which provide emission in the NIR region. PL spectra were excited with a 480 nm laser diode.

3.2 Structural Characterizations

The prepared Cd₃P₂, SiO₂@QDs and PS@QDs composites were characterized using SEM and TEM to provide more direct evidence that the Cd₃P₂ QDs were encapsulated in the

micro-spheres. Fig. 2a displays a typical SEM image of $\text{SiO}_2@$ QDs. As may be expected, SiO_2 spheres of 40-60 nm in diameter are observed, which is a typical characteristic resulting from the Stöber method.³⁷ The addition of Cd_3P_2 QDs seems not to affect the hydrolysis of TEOS in the presence of ammonium hydroxide. The SEM morphology of $\text{PS}@$ QDs is shown in Fig. 2b. Monodisperse micro-spheres of about 150 nm obtained by the two-stage copolymerization of styrene and QDs in ethanol are found. With an increase in the ratio of styrene to AIBN, the average size of the $\text{PS}@$ QDs micro-spheres becomes larger, while the size distribution does not appear to deteriorate. Fig. 2c and 2d present the TEM images of the micro-sphere cross-sections for $\text{SiO}_2@$ QDs and $\text{PS}@$ QDs, respectively. As is clearly seen, the black dots representing Cd_3P_2 QDs are embedded in the internal structure of the SiO_2 spheres. The shape of the $\text{SiO}_2@$ QD particles is generally spherical and their average diameter lies still in the same range. Similar to the observation as made from the SEM images, the size distribution of the SiO_2 micrometer-spheres is reasonably uniform. Although there are some aggregates of QDs present after they had been incorporated in the SiO_2 , no independent QDs were observed to remain separately from SiO_2 particles. No QDs could be observed to be presented on the surface of SiO_2 beads or PS micro-spheres. This suggests that the Cd_3P_2 QDs are primarily encapsulated in the micro-sized SiO_2 beads since no further QD residue could be retrieved from the solution during the centrifugation step. No great amount of aggregation was observed to occur in case of $\text{PS}@$ QDs. As shown in Fig. 2d, while the QDs are uniformly distributed in PS micro-spheres the shape of the micro-spheres changes to that of an elliptical form due to the cutting effects. The phase of the QDs imbedded in the composite was also studied by analysis of the maps of the energy dispersive spectra (EDS) and the selected area electron diffraction (SAED). The mapping image, EDS profile and data for the elemental percentages are presented in the supporting

information (Fig. S1, S2, and Table S2, S3). The result demonstrates that the black dots embedded in the micro-beads are indeed Cd_3P_2 . Fig. 2e presents the SAED pattern of $\text{SiO}_2@\text{QDs}$. Diffraction dots and rings can be seen in Fig. 2e which demonstrates that the sample contains multiple crystals. As has been reported, SiO_2 synthesized using the Stöber method is amorphous when the sample has not been thermally annealed.³⁷ Thus it is reasonable to suggest that the presence of crystalline material derives from the presence of the Cd_3P_2 QDs. Despite the fact that the diffraction rings in the SAED pattern of the $\text{PS}@\text{QDs}$ sample are not well resolved, as may be seen from the inset of Fig. 2d, the high-resolution TEM (HRTEM) image presented in Fig. 2f displays ample evidence of well resolved lattices. The d-spacings estimated to be 0.26 and 0.15 nm are consistent with d_{422} and d_{444} of cubic cadmium phosphide, respectively. This result is also consistent with our previous findings where a low temperature synthesis was capable of affording the production of cubic cadmium phosphide.¹⁰

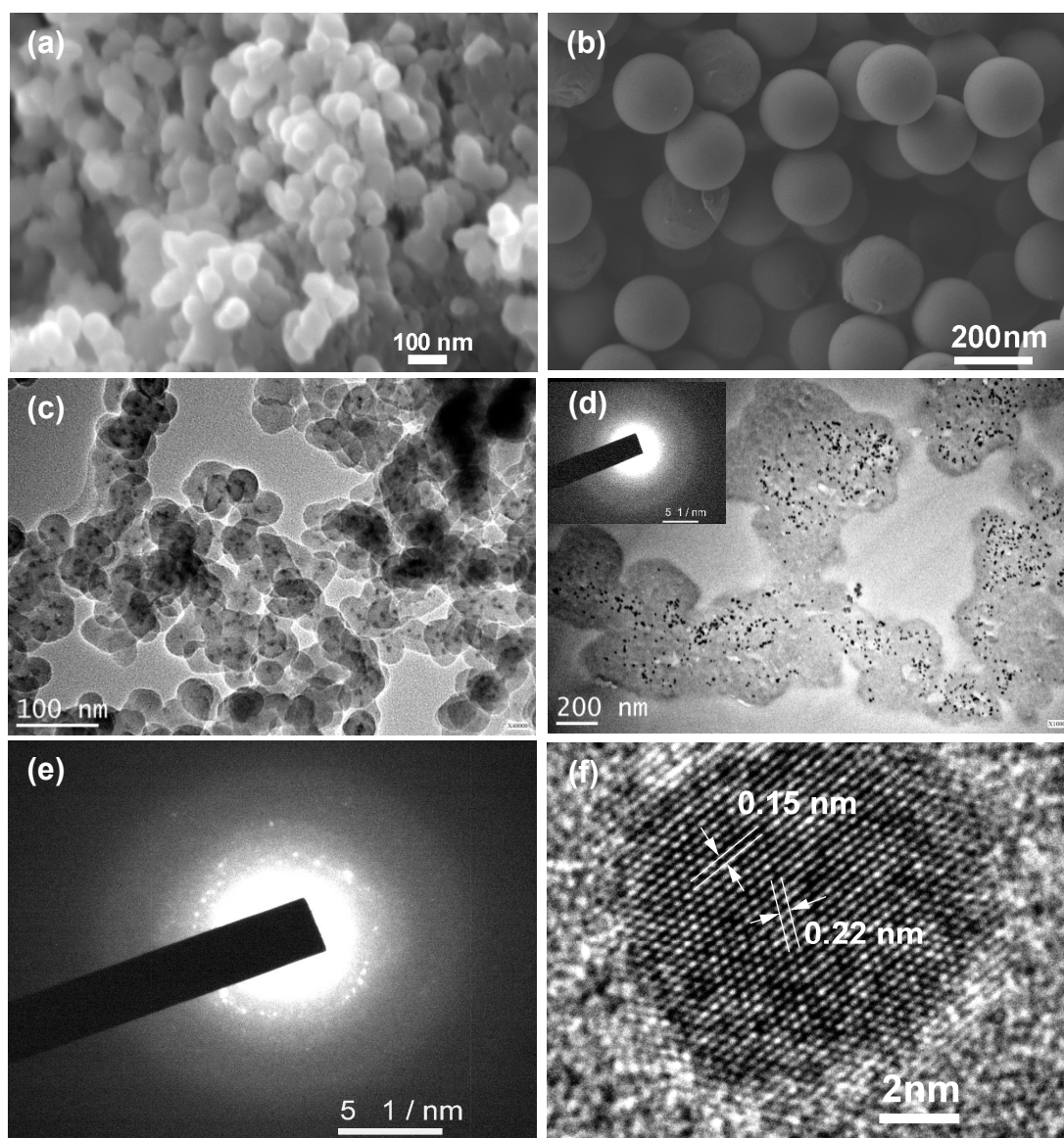


Fig.2 (a, b) SEM images of SiO₂@QDs (a) and PS@QDs (b) micro-spheres; (c, d) TEM images (cross-section) of SiO₂@QDs (c) and PS@QDs (d); Inset in Fig. 2d is the SAED pattern of PS@QDs. (e) The SAED pattern of SiO₂@QDs corresponding the area in Fig. 2c; (f) HRTEM of an embedded NIR emissive QD particle in a PS micro-sphere.

To further study the phase of the synthesized samples powders of neat Cd₃P₂ QDs, PS micro-spheres, SiO₂ nano-beads, SiO₂@QDs and PS@QDs were analyzed by powder X-ray diffraction (XRD). As can be seen in Fig. 3a, Cd₃P₂ QDs display notable diffraction peaks at 2θ values of around 28.9° and 41.7° which can be indexed to the (222) and (422) planes of cubic Cd₃P₂. The SiO₂ beads prepared via Stöber method do not show any notable XRD peaks, again demonstrating the amorphous nature of these beads. In the composite SiO₂@QDs material two peaks assigned to Cd₃P₂, while faint, could still be observed. The peaks are denoted by the arrows in Fig. 3a. This again suggests the successful incorporation of QDs into the SiO₂ beads as previously evidenced by the TEM analysis. In the case of PS@QDs the two peaks are clearly more visible as illustrated in Fig. 3b and hence the XRD study further confirms the presence of QDs in the prepared composites.

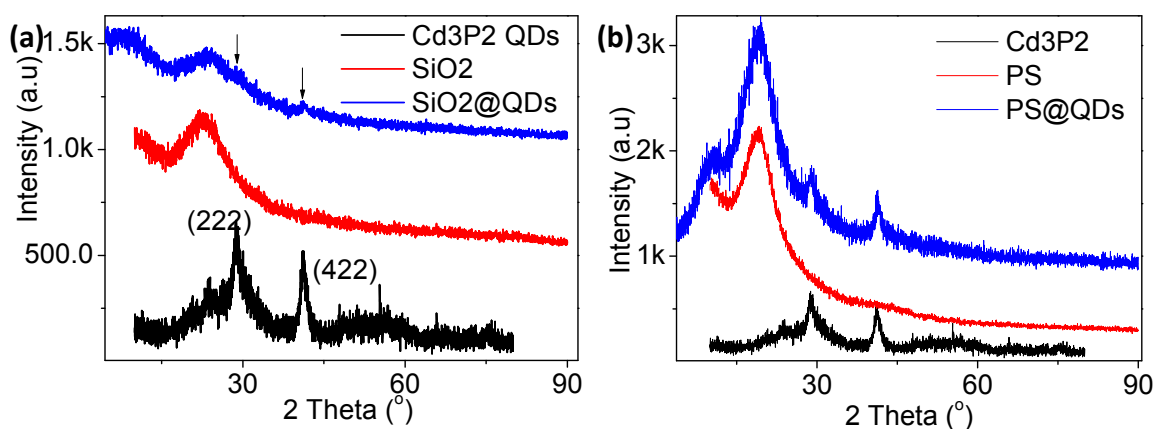


Fig.3 (a) XRD patterns for QDs, PS and PS@QDs; (b) XRD patterns for QDs, SiO₂ and SiO₂@QDs

3.3 Optical and Chemical Stability Study

As has previously been reported, the stability of Cd_3P_2 QDs is sensitive to their surface structure as well as their surrounding environments.¹⁰ Therefore, it is necessary to evaluate both the chemical and photostability of the Cd_3P_2 upon exposure to the PBS solution. Two representative micro-PL images of the photo-etched samples ($\text{PS}@ \text{Cd}_3\text{P}_2$ and $\text{SiO}_2@ \text{Cd}_3\text{P}_2$) were captured after illumination for a period of 24 hrs under UV illumination; these images are shown in Fig. 4a and 4b, respectively. The photo-etching experiments were performed by dispersing the samples in PBS solutions, and exposing the dispersions to UV irradiation (~ 365 nm). Samples were subsequently collected by centrifugation and observed under a fluorescence microscope. The initial PL images for the samples of $\text{PS}@ \text{Cd}_3\text{P}_2$ and $\text{SiO}_2@ \text{Cd}_3\text{P}_2$ are displayed in Fig. 4c and 4d, respectively. By comparing Fig. 4a (4c) and 4b (4d), it is obvious that the fluorescence of $\text{PS}@ \text{Cd}_3\text{P}_2$ fades more significantly than that of $\text{SiO}_2@ \text{Cd}_3\text{P}_2$ after 24 hrs of illumination although the sample $\text{PS}@ \text{Cd}_3\text{P}_2$ exhibits stronger photoluminescence at the starting stage. The $\text{SiO}_2@ \text{Cd}_3\text{P}_2$ remains luminescent throughout the test with only a 10% loss in intensity. Fig. 4e shows the variations of the PL intensity sampled at different stages. These tests clearly show that with respect to long-term stability it is more beneficial to employ $\text{SiO}_2@ \text{Cd}_3\text{P}_2$ for applications where the tracking of biological tissues is required as the silica shell appears to enhance the stability of the Cd_3P_2 QDs and i.e. is more resistant when placed into quite hostile environments.

To determine the potential cytotoxicity of the Cd_3P_2 -based composite particles, the release of Cd^{2+} after the samples were incubated with PBS solution were measured. In Fig. 4f the concentration dependence of Cd^{2+} on the incubation time for neat QDs, $\text{SiO}_2@ \text{Cd}_3\text{P}_2$ and $\text{PS}@ \text{Cd}_3\text{P}_2$ is presented. It was found that the neat Cd_3P_2 QDs are almost completely decomposed after 10 days, and a maximum in the concentration profile (47.6 ppm) was obtained. In contrast, the composite spheres are much more stable which is evidenced by the fact that the

concentration of Cd^{2+} released is quite low (0.5~7.5 ppm) even after two months. It is especially notable that in the case of $\text{SiO}_2@\text{Cd}_3\text{P}_2$ the ratio of Cd^{2+} released with respect to that of the neat Cd_3P_2 QDs is only 0.46%, the result of which means that the stability of Cd_3P_2 coated with SiO_2 beads is enhanced by 215 times. We have also found that the $\text{PS}@\text{Cd}_3\text{P}_2$ composite is not as stable as that of $\text{SiO}_2@\text{Cd}_3\text{P}_2$. The reason may lie in the nature of the surface of Cd_3P_2 and additionally in the shell materials.⁴³ This study demonstrates that a low toxicity can be obtained if Cd_3P_2 QDs are encapsulated into SiO_2 nano-beads. In addition the results indicate that the innocuous silica shells can prevent the QDs from undergoing decomposition and effectively avoid the release of heavy metal ions, thereby confirming our hypothesis that this type of luminescent silica nano-sphere is indeed promising for bio-analytical assays.

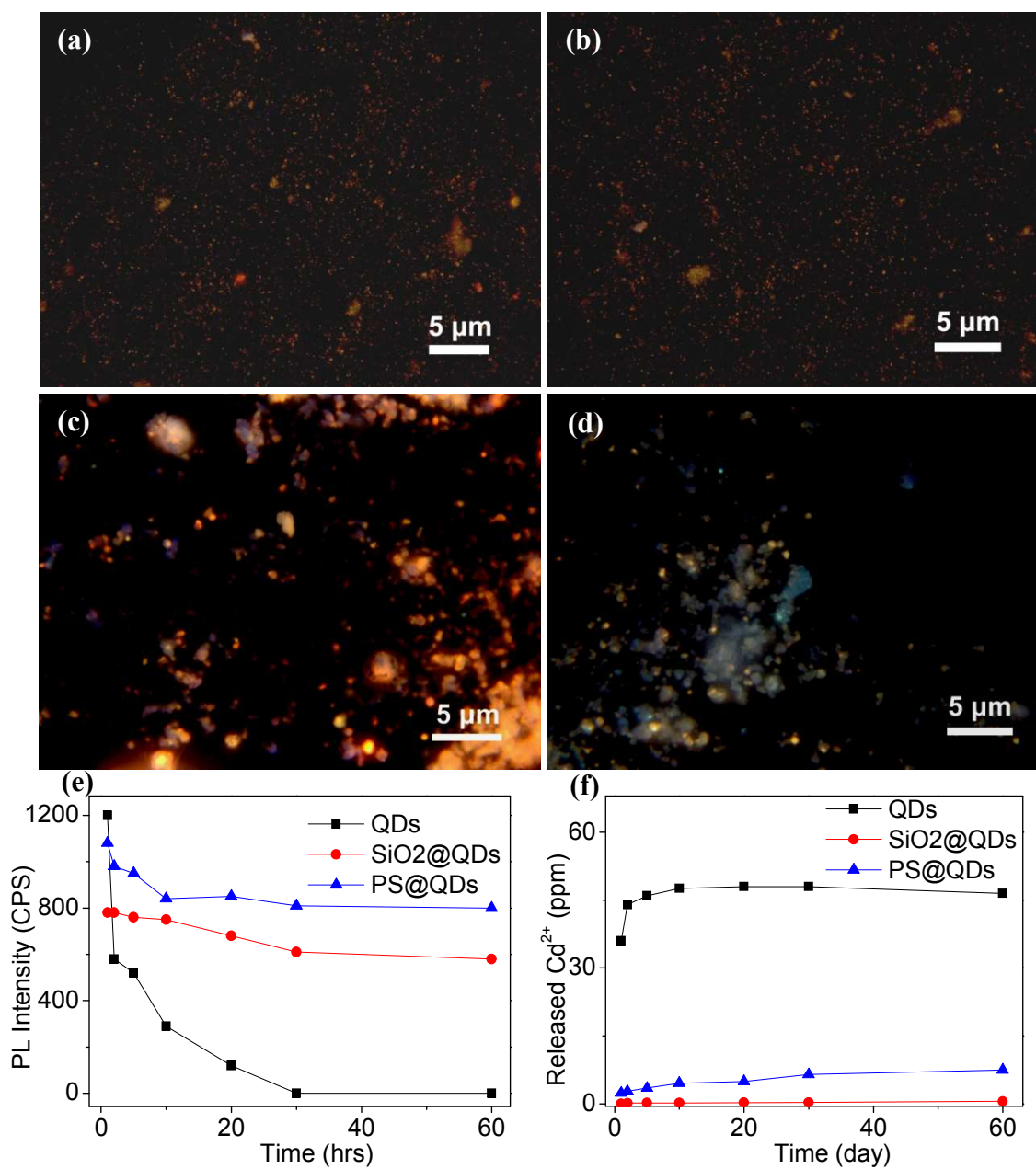


Fig.4 (a, b, c and d) Fluorescence microscopic images of PS@QDs (a, b) and SiO₂@QDs (c, d) sampled at the initial (a, c) and after incubation with PBS for 24 hrs (b, d); (e) Variation of the PL intensity as a function of the incubation time; (f) Variation of the Cd²⁺ concentration as a function of the incubation time at room temperature.

3.4 Bio-labelling Investigation

To assess the viability of using Cd_3P_2 -based QDs as fluorescent probes for bio-labelling, incubated living cells were treated with the prepared fluorescent particles in simulated physiological fluids. A period of incubation at 37°C was followed by removal of the medium followed by washing in PBS. Fluorescence microscopy images of the samples labelled using the prepared composites are displayed in Fig. 5a and 5c. For comparison the differential interference contrast (DIC) images of LoVo cells are also displayed in Fig. 5b and 5d. From the images it can be clearly seen that both composites can specifically detect the LoVo cells, especially when cells grow into aggregates or adhere to the wall of the petri dishes. The cell aggregates labelled by the fluorescent beads are more easily observed. Herein, we cannot exclude the free fluorescent beads that are intracellularly distributed, however we did find single cell in ellipse shape labelled in Fig. 5a or 5c. This demonstrates both types of beads can be taken up internally by LoVo cells. It is also observed that composite beads of $\text{PS}@ \text{Cd}_3\text{P}_2$ were distributed throughout the cells, and exhibit stronger fluorescence than $\text{SiO}_2@ \text{Cd}_3\text{P}_2$. This can be explained by the higher quantum yield when Cd_3P_2 QDs were encapsulated in PS substrate.^{43,44} However, $\text{SiO}_2@ \text{Cd}_3\text{P}_2$ nano-beads are better at yielding resolved single cells. As can be seen by comparison of the bright field image in Fig. 5d, which was incubated with $\text{SiO}_2@ \text{Cd}_3\text{P}_2$, with the corresponding fluorescent picture numerous red dots which indicate the co-localization of the internalized $\text{SiO}_2@ \text{Cd}_3\text{P}_2$ nano-beads and LoVo cells are presented. Furthermore, the nearly one-to-one correspondence between cells shown in both bright field under fluorescence mode and DIC images not only demonstrates that the $\text{SiO}_2@ \text{Cd}_3\text{P}_2$ particles are still optically active, but also manifests the feasibility of using the current composite QDs for cancer cell detection. Comparatively, in a controlled experiment using the non-encapsulated QDs only weak

fluorescence was observed after 6 hrs incubation (see Fig. S3 in the supporting information), indicating that the QDs were not stable in the cells compared to that of the $\text{SiO}_2@\text{Cd}_3\text{P}_2$ and $\text{PS}@\text{Cd}_3\text{P}_2$ materials. It has been reported that QDs can be designed to interact with a biological sample through electrostatic or hydrogen bonding once modifiable to suit their target.⁴⁴ Herein, the $\text{SiO}_2@\text{Cd}_3\text{P}_2$ has more hydrophilic groups (e.g., -OH) and would thus be expected to interact with the surface of most cells preferentially through an active endocytic or phagocytic mechanism that is temperature and energy dependent.⁴⁵

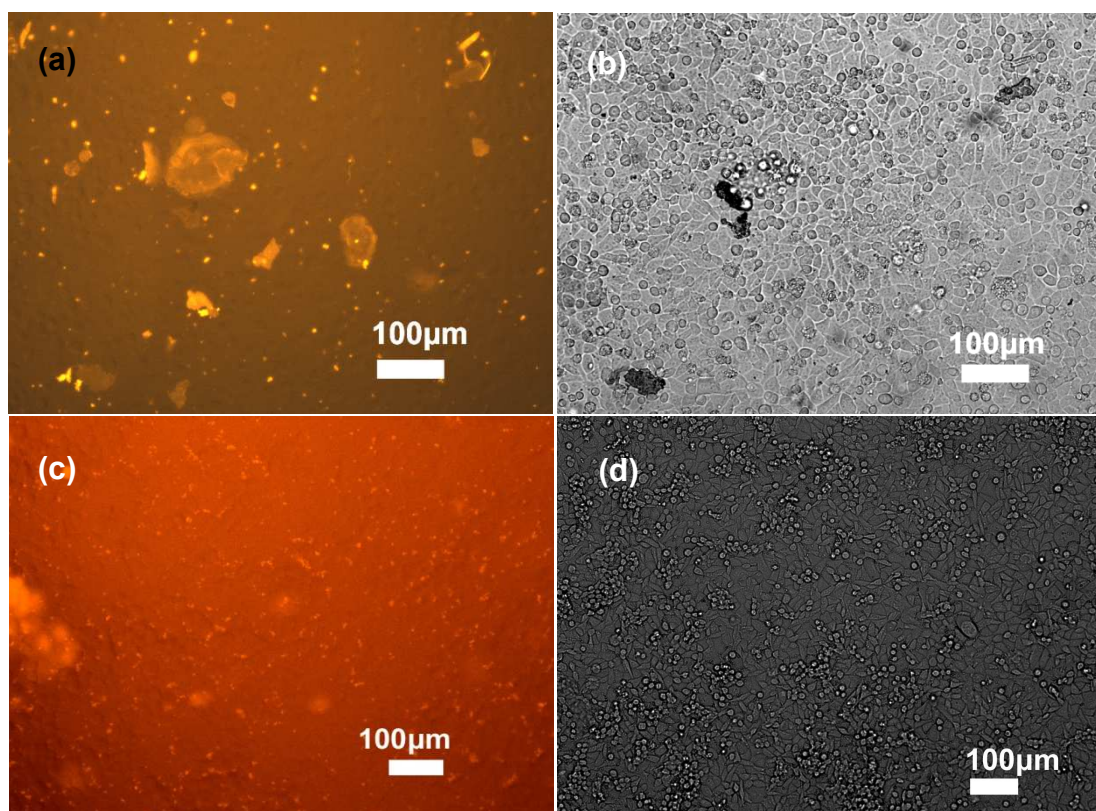


Fig.5 Fluorescence images (left row, taken under UV light) and bright field images (DIC, right row) of LoVo cells obtained after incubation with the $\text{PS}@\text{QDs}$ composite (a, b) and $\text{SiO}_2@\text{QDs}$

(c, d). The fluorescent particles were cultured with LoVo cells to track the intracellular uptake at 6 hrs transfection.

4. Conclusion

In conclusion, both polymeric and inorganic fluorescent probes have been successfully prepared by embedding Cd₃P₂ QDs in PS micro-spheres and SiO₂ nano-beads via a two-step co-polymerization and a revised Stöber method. The optical properties of the two types of composite beads resemble those of the QDs which show a size-dependence optical response spanning from the visible to the NIR spectral region. PS@Cd₃P₂ delivers a stronger photoluminescence, but the stability is inferior and the release of Cd²⁺ much faster than that of SiO₂@Cd₃P₂ upon exposure to the PBS solution. After incubation for 60 days, the released amount of Cd is only 0.46% of the whole Cd contained in the Cd₃P₂ QDs. The present work provides new routes for coating Cd₃P₂ QDs with different materials and their potential application as biological probes, e.g. for cancer cell detection, has been shown.

ASSOCIATED CONTENT

Supporting Information Available: The supplementary materials including TEM and EDS mapping spectra, and fluorescence microscopic images of LoVo cells labelled with neat Cd₃P₂ QDs were given in supporting information. This material is available free of charge via the Internet at <http://pubs.rsc.org>.

AUTHOR INFORMATION

*Corresponding_Author: Shiding Miao †

† Anhui Key Lab of Controllable Chemical Reaction & Material Chemical Engineering, School of Chemical Engineering, Hefei University of Technology, Tunxi Road. 193, Hefei, Anhui Prov., 230009, China

Tel: (+) 86-551-62901560, Fax: (+) 86-551-62901450, E-mail: miaosd@iccas.ac.cn (S. Miao)

ACKNOWLEDGMENT

This research was financially supported by the National Natural Science Foundation of China (21103039), Research Fund for the Doctoral Program of Higher Education of China (20110111120008), Anhui Provincial Natural Science Foundation for Distinguished Young Scholars (J2014KJZS0202) and the Beijing National Laboratory for Molecular Sciences (J2014AKYQ0041). Professor A. Eychmüller acknowledges a visiting professorship for senior international scientists of Chinese Academy of Sciences (CAS).

Notes and References

- 1 I. L. Medintz, H. T. Uyeda, E. R. Goldman, H. Mattoussi, *Nat. Mater.*, 2005, **4**, 435-446.
- 2 S. Miao, S. G. Hickey, C. Waurisch, V. Lesnyak, T. Otto, B. Rellinghaus, A. Eychmüller, *Acs Nano*, 2012, **6**, 7059-7065.
- 3 S. B. Sharma, P. Paliwal, M. Kumar, *J. Phys. Chem. Solids.*, 1990, **51**, 35-39.
- 4 W. Zdanowicz, L. Zdanowicz, *Annu. Rev. Mater. Sci.*, 1975, **5**, 301-328.
- 5 M. Green, P. O'Brien, *Chem. Mater.*, 2001, **13**, 4500-4505.
- 6 P. K. Khanna, N. Singh, P. More, *Curr. Appl. Phys.*, 2010, **10**, 84-88.
- 7 S. J. Radautsa, E. K. Arushano, A. N. Nateprov, D. A. Oleinik, *Status. Solidi. A.*, 1974, **25**, K57-K60

- 8 P. Lin-Chung, *Phys. Status. Solidi. B.*, 1971, **47**, 33-39.
- 9 K. Sieranski, J. Szatkowski, J. Misiewicz, *Phys. Rev. B.*, 1994, **50**, 7331-7337.
- 10 S. Miao, S. G. Hickey, B. Rellinghaus, C. Waurisch, A. Eychmüller, *J. Am. Chem. Soc.*, 2010, **132**, 5613-5616.
- 11 Z. Chen, X. Ren, X. Meng, L. Tan, D. Chen, F. Tang, *Biosens. Bioelectron.*, 2013, **44**, 204-209.
- 12 F. Wu, Q. Cui, Z. Qiu, C. Liu, H. Zhang, W. Shen, M. Wang, *ACS. Appl. Mater. Inter.*, 2013, **5**, 3246-54.
- 13 J. Li, J. J. Zhu, *Analyst.*, 2013, **138**, 2506-15.
- 14 T. Pellegrino, L. Manna, S. Kudera, T. Liedl, D. Koktysh, A.L. Rogach, S. Keller, J. Rädler, G. Natile, W.J. Parak, *Nano. Lett.*, 2004, **4**, 703-707.
- 15 S. T. Selvan, T. T. Y. Tan, D. K. Yi, N.R. Jana, *Langmuir*, 2010, **26**, 11631-11641.
- 16 Q. Liu, L. Wang, A. Xiao, H. Yu, Q. Tan, J. Ding, C. Yu, *Macromol. Symp.*, 2008, **261**, 113-120.
- 17 R. F. Meyer, W. B. Rogers, M. T. McClendon, J. C. Crocker, *Langmuir*, 2010, **26**, 14479-14487.
- 18 S. K. Yen, D. Janczewski, J. L. Lakshmi, S. B. Dolmanan, S. Tripathy, V. H. B. Ho, V. Vijayaragavan, A. Hariharan, *ACS Nano* 2013, **7**, 6796-6805.
- 19 H. Fudouzi, Y. N. Xia, *Adv. Mater.*, 2003, **15**, 892-896.
- 20 H. Yoon, Y. M. Rhym, S. E. Shim, *Colloid. Poly. Sci.*, 2013, **291**, 1155-1162.
- 21 Y. H. Lee, C. S. Tseng, Y. L. Wei, *J. Mater. Res.*, 2012, **27**, 2829-2836.
- 22 Y. Chen, J. Cho, A. Young, T. A. Taton, *Langmuir*, 2007, **23**, 7491-7497.

- 23 F. Song, P. S. Tang, H. Durst, D. T. Cramb, W. C. W. Chan, *Angew. Chem. Int. Ed.*, 2012, **51**, 8773-8777.
- 24 C. Mader, I. Schnöll-Bitai, *Macromol. Chem. Phys.*, 2005, **206**, 649-657.
- 25 M. Kohri, S. Uzawa, A. Kobayashi, H. Fukushima, T. Taniguchi, T. Nakahira, *Polym. J.*, 2013, **45**, 354-358.
- 26 F. Tronc, M. Li, J. P. Lu, M. A. Winnik, B. L. Kaul, J. C. Graciet, *J. Polym. Sci. Pol. Chem.*, 2003, **41**, 766-778.
- 27 L. P. Ramirez, K. Landfester, *Macromol. Chem. Phys.*, 2003, **204**, 22-31.
- 28 J. S. Song, M. A. Winnik, *Macromolecules.*, 2005, **38**, 8300-8307.
- 29 R. Koole, M. M. van Schooneveld, J. Hilhorst, C. d. M. Donega, D. C. t Hart, A. van Blaaderen, D. Vanmaekelbergh, A. Meijerink, *Chem. Mater.*, 2008, **20**, 2503-2512.
- 30 Y. Yang, W. N. Li, Y. S. Luo, H. M. Xiao, S. Y. Fu, Y. W. Mai, *Polymer.*, 2010, **51**, 2755-2762.
- 31 A. Zhang, P. Yang, N. Murase, *J. Nanosci. Nanotechno.*, 2013, **13**, 2993-2998.
- 32 S.T.Selvan, *Biointerphases*, 2010, **5**, FA110–FA115.
- 33 H. Chen, S. Cui, Z. Tu, Y. Gu, X. Chi, *J. Fluoresc.*, 2012, **22**, 699-706.
- 34 X. Zhou, X. Wang, F. Liu, Z. Chen, A. Kasuya, *Curr. Nanosci.*, 2008, **4**, 88-91.
- 35 R. Han, M. Yu, Q. Zheng, L. Wang, Y. Hong, Y. Sha, *Langmuir*, 2009, **25**, 12250-12255.
- 36 Y. Zhu, Z. Li, M. Chen, H. M. Cooper, G. Q. Lu, Z. P. Xu, *Chem. Mater.*, 2012, **24**, 421-423.
- 37 W. Stoeber, A. Fink, E. Bohn, *J. Colloid. Interf. Sci.*, 1968, **26**, 62-9.
- 38 F. Darro, A. Kruczynski, C. Etievant, J. Martinez, J. L. Pasteels, R. Kiss, *Cytometry*, 1993, **14**, 783-92.

- 39 H. W. Duan, S. M. Nie, *J. Am. Chem. Soc.*, 2007, **129**, 3333-3338.
- 40 R. Wang, C. I. Ratcliffe, X. Wu, O. Voznyy, Y. Tao, K. Yu, *J. Phys. Chem.C.*, 2009, **113**, 17979-17982.
- 41 Z. Yang, I. Sokolik, F. E. Karasz, *Macromolecules*, 1993, **26**, 1188-1190.
- 42 T. Uchihara, M. Shiroma, K. Ishimine, Y. Tarnaki, *J.Photochem. Photobiolo. A.*, 2010, **213**, 93-100.
- 43 H. Zhang, P. Sun, C. Liu, H. Gao, L. Xu, J. Fang, M. Wang, J. Liu, S. Xu, *Luminescence*, 2011, **26**, 86-92.
- 44 M. Wilchek, E. A. Bayer, *Trends. Biochem.Sci.*, 1989, **14**, 408-12.
- 45 M. Visentin, M. P. Simula, F. Sartor, A. Petrucco, V. DeRe, G. Toffoli, *Inter. J. Oncolo.*, 2009, **34**, 1281-1289.